International Journal of Chemical, Materials and Biomolecular Sciences
ISSN: 2415-6620
Vol:7, No:4, 2013

CFD Study of Turbine Submergence Effects on Aeration of a Stirred Tank

Achouri Ryma, Hatem Dhaouadi, Hatem Mhiri, and Philippe Bournot

***Abstract*—**For many chemical and biological processes, the understanding of the mixing phenomenon and flow behavior in a stirred tank is of major importance. A three-dimensional numerical study was performed using the software Fluent, to study the flow field in a stirred tank with a Rushton turbine. In this work, we first studied the flow generated in the tank with a Rushton turbine. Then, we studied the effect of the variation of turbine's submergence on the thermodynamic quantities defining the flow field. For that, four submergences were considered, while maintaining the same rotational speed (N=250rpm). This work intends to optimize the aeration performances of a Rushton turbine in a stirred tank.

***Keywords*—**Aeration, CFD, mixing, Rushton turbine, submergence.

I. Introduction

THE mixing operation is one of the most universal. Difficult to find an industry that does not include agitation to one of its stages. This is also the variety of users that contributed to the development of agitation tools. The stirring process can have multiple purposes. It is usually a mixture of two phases (gas / liquid, gas / solid or liquid / solid) or three phase (gas / liquid / solid). Several experimental investigations were chained followed by numerical studies of fluid mechanics. CFD technology is complementary to the theoretical and experimental results despite the development of digital computers. Many years ago, researches began to focus on mixing and its industrial applications [1]. Despite the complexity of this field, in recent years several attempts have been made to develop computational models for gas-liquid flows in stirred vessels [2]-[5]. Several experimental investigations were led, followed by numerical studies of fluid mechanics [6]-[11]. Many other researchers were interested by the geometrical variation of the stirrer or the tank [12], [13]. In general, the improvement of the performance of an agitator in a tank requires a complex structure and an operation at additional cost. Therefore a better understanding of the flow generated by the turbine is required to make further design improvements. The numerical study of fluid dynamics (CFD) can provide more information on the phenomena taking place in the tank, as well as on the dispersion of air in this type of mixing device. This paper presents our recent efforts to model the turbulent flow in a stirred tank with a Rushton turbine, and to put into evidence the variation of the hydrodynamic parameters of our field with the variation of impeller submergence and with impeller rotational speed. We used the Euler-Euler multiphase model and the turbulence model k-ε standard available in Fluent to describe the flow field in this type of turbine and also to study its performances.

Ryma Achouri and Hatem Mhiri are with the UTTPI, National Engineering School of Monastir, Tunisia (phone: 0021625387105; fax: (+216) 73 50 05 14; e-mail: ryma_achouri@yahoo.fr; hatem.mhiri@enim.rnu.tn).
Hatem Dhaouadi is with University of Monastir, Sciences University, UR1204- Applied Chemistry Environnement (e-mail: hatem.dhaouadi@fsm.rnu.tn).
Philippe Bournot is with IUSTI, UMR CNRS 6595, 5 rue Enrico Fermi, Technopole de Château-Gombert, 1303 Marseille, FRANCE (e-mail: bournot@univmed.fr).

II. CFD Modeling

A. Studied Field

The studied field is a flat bottomed and an unbaffled tank, having a Rushton turbine with 6 blades as a mixer. The diameter of the tank, T, is equal to 0.36 m, height H is equal to five quarts of T (H = 5/4T = 0.45 m), and the water level in the tank is h equal to three quarts of T (h = 3/4T = 0.27 m). The geometry of our field is represented in Fig. 1, and the dimensions of the Rushton turbine are resumed in Table I.

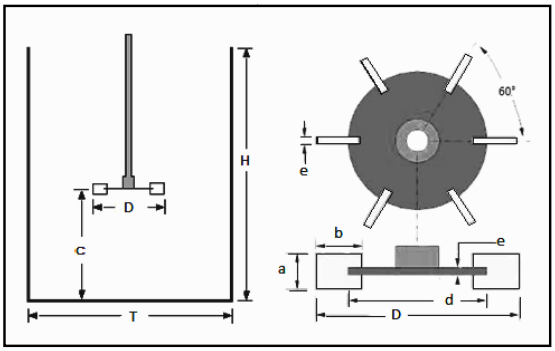

Fig. 1 Dimensions of the studied field

B. Mesh and Boundary Conditions

The studied area, as we can see, is symmetric. That is why in this work, we will be interested in only the one sixth of the configuration. This method offers a significant time savings and lower operating costs due to the precision of the adopted mesh. After grid independence study, we chose the mesh represented in Fig. 2. To create the computational domain, we used the software "GAMBIT", which allows us to mesh in two or three-dimensional geometric shapes. A boundary condition, "Moving Reference Frame", is used in the region of rotation around the turbine with a rotational speed N=250 rpm. The

pressure at the top of the tank is 1 atm; the boundary condition used is "pressure outlet". No slip condition was used in the area of the walls (no slip boundary) and treatment near the walls is standard. Air is drawn directly from the free surface of the tank which is due to depression generated behind the blades during rotation of the turbine.

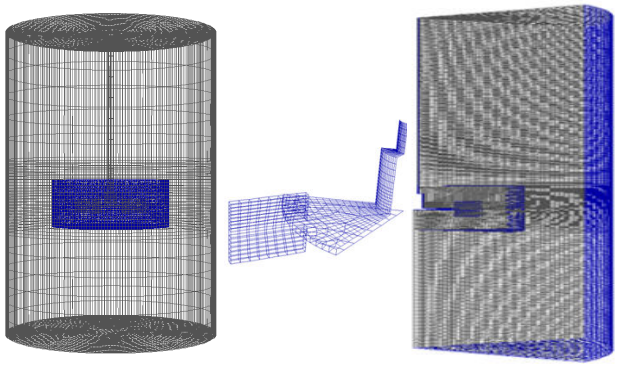

Fig. 2 Mesh of the studied field

C. Governing Equations

In order to study the flow in our configuration and the various thermodynamic quantities characterizing it, we used a simulation model and the Euler-Euler multiphase. Unlike other models, the Euler model solves equations of transport and continuity for each phase. The coupling is then achieved through pressure and heat transfer coefficients between phases. In our case, a three-dimensional simulation was performed for an air-water multiphase system. The model MRF (Moving Reference Frame) was used to simulate the different interactions between the rotating turbine and the tank and its walls. The turbulence generated by the turbine is modeled using the turbulence model k-ε standard. This model is suitable for flows with fully developed turbulence (high Reynolds number). The details of the turbulence model, as well as those of the MRF model, and the equations governing these models will be discussed.

- *Conservation Equations:*

The governing equations for an uncompressible fluid can be written as;

$$\frac{\partial \rho}{\partial t}+\frac{\partial}{\partial x_i}\left(\rho u_i\right)=0 \tag{1}$$

$$\frac{\partial}{\partial t}\left(\rho u_i\right)+\frac{\partial}{\partial x_j}\left(\rho u_i u_j\right)=-\frac{\partial P}{\partial x_i}\left(\rho u_i\right)+\frac{\partial}{\partial x_j}\left[\mu\left(\frac{\partial u_i}{\partial x_j}+\frac{\partial u_j}{\partial x_i}\right)\right]+\frac{\partial}{\partial x_j}\left(-\rho\overline{u_i' u_j'}\right) \tag{2}$$

Where the velocity components are divided into the mean $\overline{u_i}$ and the fluctuating u_i' velocities. These two components are related to each other by the following equation:

$$u_i=\overline{u_i}+u_i' \tag{3}$$

Equations (1) and (2) are called Reynolds-Averaged Navier-Stokes (RANS) equations. The Reynolds stress term $R_{ij}=\rho\overline{u_i' u_j'}$ represents the effects of turbulence and must be modeled to fully characterize equation (2).

- *MRF Model:*

The computational domain for the CFD problem was defined with respect to the rotating frame so that an arbitrary point in the CFD domain is located by a position vector $\vec{r}$ from the origin of the rotating frame. The fluid velocities can be transformed from the stationary frame to the rotating frame using the following relation:

$$\vec{v}_r=\vec{v}-\vec{u}_r \tag{4}$$

where

$$\vec{u}_r=\vec{\Omega}-\vec{r} \tag{5}$$

In these equations $\vec{u}_r$ is the "whirl" velocity (the velocity due to the moving frame), $\vec{v}_r$ is the relative velocity (velocity viewed from the rotating frame), and $\vec{v}$ is the absolute velocity (velocity viewed from the stationary frame). When the equations of motion are solved in the rotating reference frame, the acceleration of the fluid is augmented by additional terms that appear in the momentum equations. Moreover, the equations can be formulated in two different ways: Expressing the momentum equations using the relative velocities as dependent variables (known as the relative velocity formulation), or expressing the momentum equations using the absolute velocities as dependent variables in the momentum equations (known as the absolute velocity formulation).

- *The Standard k–ε Model:*

The standard k- ε model is a semi-empirical model based on model transport equations for the turbulence kinetic energy (k) and its dissipation rate (ε). The model transport equation for k is derived from the exact equation, while the model transport equation for ε was obtained using physical reasoning and bears little resemblance to its mathematically exact counterpart. The turbulence kinetic energy, k, and its rate of dissipation, ε, are obtained from the following transport equations:

TABLE I
DIMENSIONS OF THE RUSHTON TURBINE

Designation	Variable	Value (m)
D	Impeller Diameter	0.1243
d	Turbine's disk diameter	0.0843
E	Thickness of the turbine's disk	0.002
L_p	Blade Length	0.025
l_p	Blade width	0.02
e_p	blade thickness	0.002

$$\frac{\partial(\rho k)}{\partial t}+\frac{\partial(\rho k\overline{U_i})}{\partial x_i}=\frac{\partial}{\partial x_j}\left[\left(\mu+\frac{\mu_t}{\sigma_k}\right)\frac{\partial k}{\partial x_j}\right]+G_k + G_b-(\rho\varepsilon+Y_M) \quad (6)$$

And

$$\frac{\partial(\rho\varepsilon)}{\partial t}+\frac{\partial(\rho\varepsilon\overline{U_i})}{\partial x_i}=\frac{\partial}{\partial x_j}\left[\left(\mu+\frac{\mu_t}{\sigma_\varepsilon}\right)\frac{\partial\varepsilon}{\partial x_j}\right]+ C_{1\varepsilon}\frac{\varepsilon}{k}(G_k+C_{3\varepsilon}G_b)-C_{2\varepsilon}\rho\frac{\varepsilon^2}{k} \quad (7)$$

In these equations, G_k represents the generation of turbulence kinetic energy due to the mean velocity gradients, G_b is the generation of turbulence kinetic energy due to buoyancy, Y_M represents the contribution of the fluctuating dilatation in compressible turbulence to the overall dissipation rate, $C_{1\varepsilon}$, $C_{2\varepsilon}$, and $C_{3\varepsilon}$ are constants, σ_k and σ_ε are the turbulent Prandtl numbers for k and ε, respectively, and S_k and S_ε are user-defined source terms.

III. Numerical Results and Discussions

In what follows, we will present first the flow in a stirred tank with a Rushton-type turbine with a constant submergence corresponding to s = 8 cm, s is the distance between the free surface of the water and the turbine. The effect of submergence (s = 0, 2, 6 and 8 cm) will be studied in the second part, from the results established in the first part.

A. Flow Field:

In this section we will study the different aspects and phenomena taking place in a stirred tank, with a Rushton turbine with six blades, according to the simulation assumptions chosen earlier. The setting for the global study of the flow is the one corresponding to the submergence s = 8 cm. Fig. 3 shows the volume fraction of water during this time in the plan y = 0, and the progressive deformation occurring at the free surface. Note that a vortex is created gradually at the free surface to reach the level of the turbine disk. This void is immediately filled by air, which penetrates the water and incorporates it by the continual movement of the free surface. Areas, where the volume fraction of water is less than unity, confirm this finding.

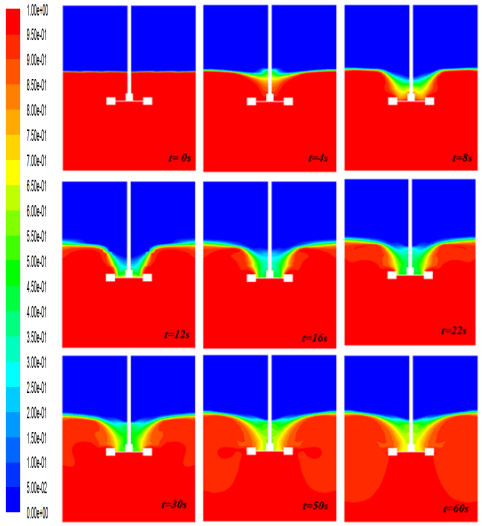

Fig. 3 Evolution of water volume fraction contours over time

Fig. 4 shows the contours of the global velocity in the tank, this figure points the maximum global velocity in the neighboring region of the blades close to 1.76 m / s. The global velocity is actually the speed of the blade tip. It is found that high global velocity zones are more spread out downstream of the blades rather than upstream. The turbine rotating in the direction of clockwise, the front of the blades are first to be in contact with water which resists to movement and thus reduces speed in this region. The effect of the walls of the tank is reflected in the decrease of the global velocity as it comes close.

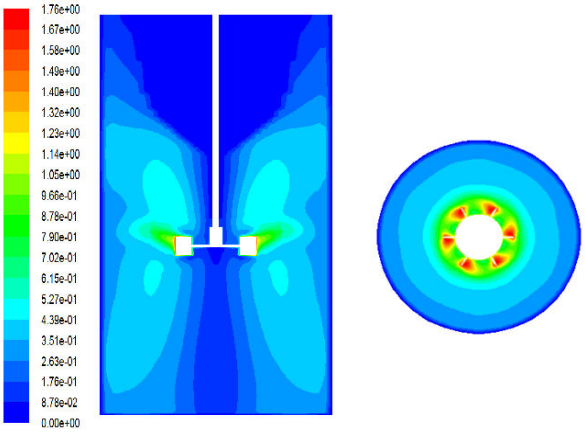

Fig. 4 Contours of global velocity

B. Effect of Turbine Submergence:

To conclude on the effect of the depth of submergence of the Rushton turbine in a stirred tank, we have developed the following four configurations: s=0 cm corresponding to C=0.27 m, s=2 cm corresponding to C=0.25 m, s=6 cm corresponding to C= 0.21 m, s=8 cm corresponding to C=0.19 m. We will adopt the same rotational speed of the turbine that is N=250 rpm. The distribution of phases when the flow is

established for each configuration is illustrated in the plan y=0, in Fig. 5.

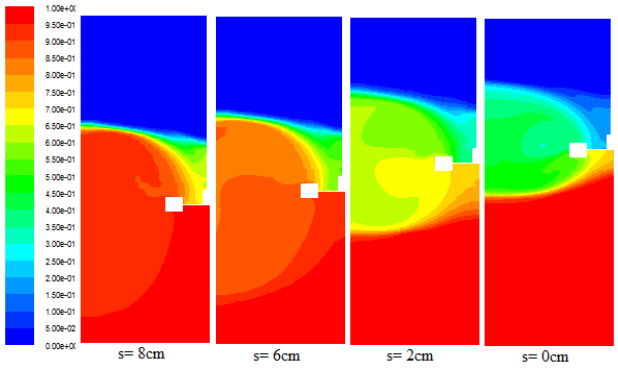

Fig. 5 Contours of phases for different submergences

We can notice that, more the agitator is located near the free surface, the more it stands at a close distance of the sky of the tank. When the half of blades of the Rushton turbine are submerged in water and the other half in the open air (s = 0cm), the rotational effect implies more water upward. This also implies that the training of the air is more important as the height of submergence is small. The contours of the global velocity are shown in Fig. 6. The water propelled by the blade of the turbine reaches the tank wall to divide it into two axial flows, one ascending and one descending. The water that goes to the bottom of the tank is mostly drawn again by the blade. A small percentage continues to flow to the bottom of the tank where, faced with the effect of the wall, recirculates up.

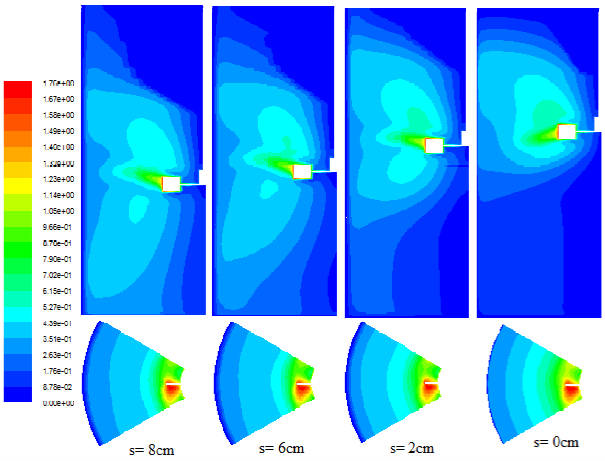

Fig. 6 Contours of global velocity in the plans y=0 and z=C

For the radial velocity, which the contours are shown in Fig. 7 (a) below, we note that the areas affected by the rotation of the turbine are more tightly around it. For s=0 cm, the fluid occupying the bottom of the tank has a very low radial motion (in the order of 2, 58 10^{-2} m/s). The maximum speed is located downstream the blade of the turbine and for different submergences.

However, these maxima depend on the configuration as shown in Fig. 7 (b). The curves of radial velocity as a function of radial position are drawn in the plane z = C and θ=5°. We see that the radial velocity have the same appearance, for the different submergences, with a small difference toward the blade tip, which is due to the closeness to the free surface of the tank and maybe the quality of mesh.

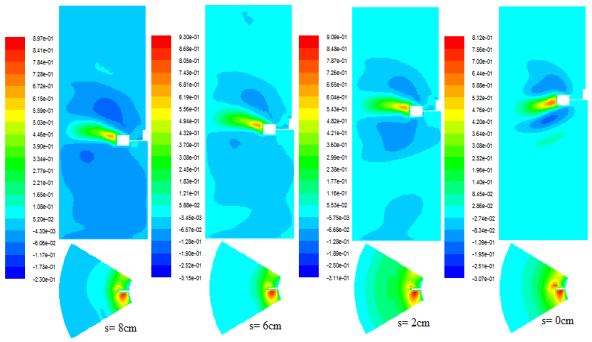

(a)

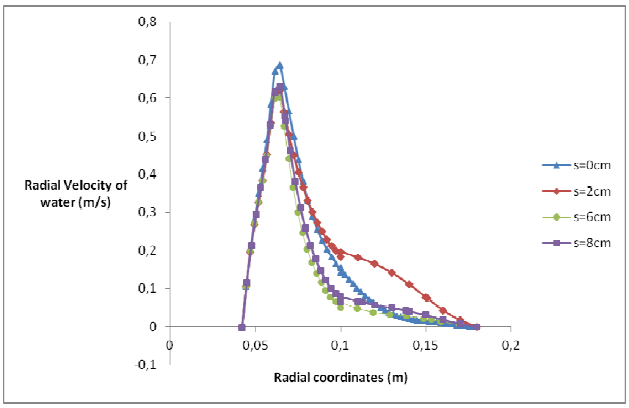

(b)

Fig. 7 (a) Contours of radial velocity for different submergences in the plans y=0 and z=C (b) evolution of the radial velocity with the radial position at z = C and θ=5° for different submergences

The fig. 8 and 9 below allow noting the similarity in the qualitative profiles of the turbulent kinetic energy k. The highest values are recorded around the blade as the turbulent kinetic energy is related not only to the velocity gradients but also to the phenomena of separation and vortex. According to the scales accompanying the contours of k, the maximum value increases with the submergence of the stirrer. For s = 8 cm and s = 6 cm, turbulent kinetic energy is greater at the top of the blade rather than at it, given the direction of the jet of water from the turbine. This finding is no longer valid when the clearance increases. The kinetic energy at the turbine is similar to that above the blade to overcome when submergence becomes zero.

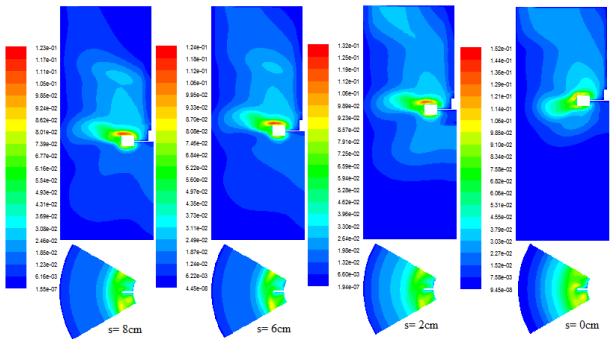

Fig. 8 Contours of turbulent kinetic energy in the plan y=0 and z=C

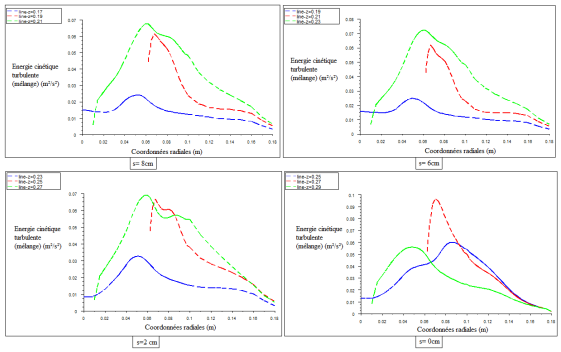

Fig. 9 Evolution of the turbulent kinetic energy for each submergence above, at and below the blades

TABLE II
THE POWER NUMBER AND THE PUMPING NUMBER FOR DIFFERENT SUBMERGENCES

S (cm)	N_P= P/ρN3D5	N_Q=Q/ND^3
0	0.86	0.16
2	1.36	0.26
6	1.943	0.36
8	2.093	0.36

Fig. 10 indicates the elevation of the maximum turbulent dissipation rate with the submergence value. We notice that large dissipations are no longer touching the bottom edge of the blade but only the top edge.

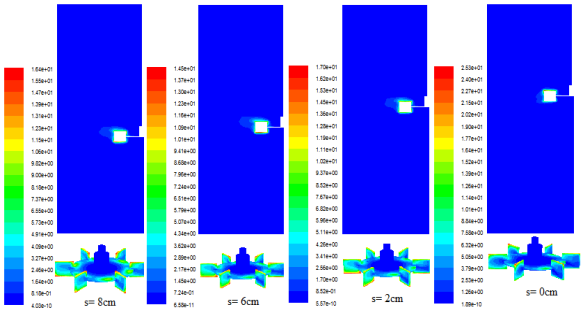

Fig. 10 Contours of turbulent dissipation rate in the plan y=0 and around the turbine

For every stirred vessel, there are quantitative and dimensionless numbers that have to be known. These numbers are the power number N_P and the pumping number N_Q. Table II summarize the increase of the value of these numbers with the increase of the submergence s, keeping the same rotational speed N=250rpm. This increase is due to the increase of power needed to rotate the turbine when its submergence is more important.

So we conclude here, that for an increased submergence of our turbine, the power number and the pumping number are increasing too. But for the same submergence (S=8 cm) we notice that the quality of mixing is better, and the aeration of our fluid is better.

In a next step, we tried to find the experimental value of the volumetric coefficient of mass transfer kLa for 4 different submersions, and for different rotational speed. Our experimental results are resumed in the fig. 11 and 12.

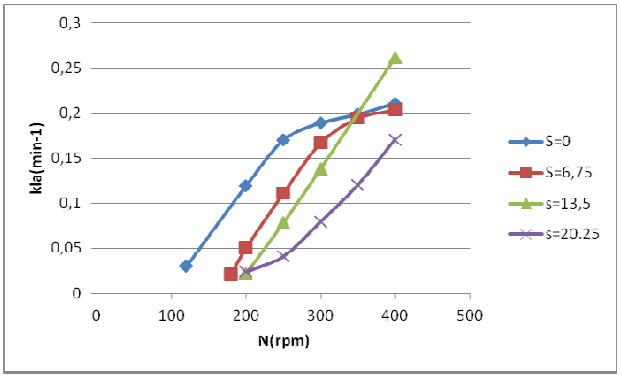

Fig. 11 kLa for differents submersions

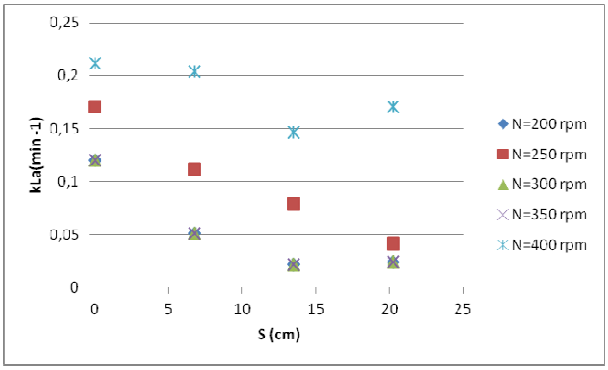

Fig. 12 k_La for different rotational speed

We conclude here that the better aeration performances are obtained for the most important rotational speed and for the lowest submergence.

IV. CONCLUSION

A numerical study of a stirred tank was developed in this work. The chosen agitator is a Rushton turbine. We first studied the flow, into the tank and also, next to the turbine. Then, we demonstrated the effect of the variation in the

turbine submergence on the generated flow. Finally, we were interested in the quantitative data characterizing a stirred vessel, which are the power number and the pumping number. We conclude that to have a good mixing of our fluid in the stirred tank, we should select the deepest submergence, but the disadvantage of this choice is the request in power. We should find the best balance between them, and try to study numerically other characterizing parameters, as the volumetric coefficient of mass transfer k_La witch give us a better idea on the aeration performances of each turbine.

REFERENCES

[1] Nagata, S. (1975) "Mixing: Principles and Applications". New York : Halstead Press.
[2] Lane G.L, Schwarz M.P. and Evans G.M. Comparison of CFD method for modeling of stirred tanks, Proc. 10th European Conference on Mixing, Delft, the Netherlands, 2000, 197-204.
[3] Ljungqvist M., Rasmuson A. Numerical Simulation of the Two-Phase Flow in an Axially Stirred Vessel," Trans IChemE, 2001, 79, Part A, pp. 533–546.
[4] Khopkar A., Aubin J., Rubio-Atoche C., Xuereb C., Le Sauze N., Bertrand J. and Ranade V.V. Flow Generated by Radial Flow Impellers: PIV Measurements and CFD Simulations. International Journal of Chemical Reactor Engineering, 2004, Vol. 2: A18
[5] Dhainaut, Marc; Tetlie, Pål; and Bech, Knut. Modeling and Experimental Study of a Stirred Tank Reactor, International Journal of Chemical Reactor Engineering, 2005, Vol. 3: A61.
[6] Ranade, V. V. (1997) "An efficient computational model for simulating flow in stirred vessels: a case of Rushton turbine," Chemical Enginering Science. Elsevier Science Ltd, Vol. 52, 24.
[7] Schafer, M., Hofken, M. and Durst, F. (1997) "Detailed LDV measurements for visualization of the flow field within a stirred tank reactor equipped with a Rushton turbine," Chem. Eng. Res. Des., Vol. 75.
[8] NG, F., et al. (1998) "Assessment of sliding mesh CFD predictions and LDA measurements of the flow in a tank stirred by a rushton impeller," Trans IChemE. Institution of Chemical Engineers, Vol. 76.
[9] Jianhua, F., Yundong, W. and Weingang, F. (2007) "Large Eddy Simulation of flow instabilities in a stirred tank generated by a rushton turbine," Chin. J. Chem Eng. Vol. 15.
[10] Zadghaffari, Ramin; Moghaddas, Jafarsadegh; and Revstedt, Johan (2009) "Study of Flow Field, Power and Mixing Time in a Two-Phase Stirred Vessel with Dual Rushton Impellers: Experimental Observation and CFD Simulation," *Chemical Product and Process Modeling*: Vol. 4: Iss. 1, Article 3.
[11] Kasat, Gopal R.; Pandit, Aniruddha B.; and Ranade, V. V. (2008) "CFD Simulation of Gas-Liquid Flows in a Reactor Stirred by Dual Rushton Turbines," International Journal of Chemical Reactor Engineering: Vol. 6: A60.
[12] Kumarsen, T. and Joshi, J.B. (2005) "Effect of impeller design on the flow pattern and mixing in stirred tanks," Chemical Engineering Journal. Elsevier.
[13] Ammar, M., et al (2009) « Etude comparative entre les différentes géométries du mobile d'agitation ». 19ème Congrès Français de Mécanique. Marseille .